Viscosity Dependence of the Local Segmental Dynamics of Anthracene-Labeled Polystyrene in Dilute Solution

Dean A. Waldow† and M. D. Ediger*

Department of Chemistry, University of Wisconsin, Madison, Wisconsin 53706

Yoshikazu Yamaguchi,‡ Yushu Matsushita, and Ichiro Noda

Department of Synthetic Chemistry, Nagoya University, Nagoya 464, Japan

Received November 21, 1990; Revised Manuscript Received January 22, 1991

ABSTRACT: The local segmental dynamics of anthracene-labeled polystyrene in dilute solution have been studied by using time-correlated single-photon counting. Six solvents covering 2 decades in viscosity were utilized. Correlation times were extracted from the orientation autocorrelation functions and determined as a function of temperature in all solvents. Under good solvent conditions, the correlation time is proportional to $\eta^{0.9}$ at constant temperature, in reasonable agreement with the $\eta^{1.0}$ prediction to the Kramers' equation in the high-friction limit. Other aspects of the results are also reasonably consistent with the assumption that the solvent acts as a viscous continuum. As noted in previous investigations, somewhat slower dynamics are observed in Θ-solvents than in good solvents. The potential barrier height for local dynamics extracted from these measurements is 11 ± 3 kJ/mol.

Introduction

Polymers have varied, interesting, and important macroscopic properties. The differences in properties shown by different polymers ultimately arise from different chemical structures. Understanding these structure–property relationships is an important theme in polymer science. The study of local segmental dynamics of polymers has a significant role to play in the understanding of structure–property relationships. Dynamics on the length scale of a few monomer units depend strongly on the details of the monomer structure and influence important material properties, e.g., T_g.

Local segmental dynamics in dilute solution play a similar role with respect to the bulk as an ideal gas does with respect to a real gas. It is useful to understand local chain motions of an isolated chain in solution before chain–chain interactions must be taken into account. The first step is to understand how the solvent influences local dynamics in dilute solution. For nonpolar systems there has been an expectation that the solvent can be successfully modeled as a viscous, structureless continuum. Kramers' theory for passage over a potential energy barrier has been applied to this problem,[1,2] with the following prediction for the lifetime of a conformational state:

$$\tau_c = A\eta(T)e^{E_a/kT} \quad (1)$$

Here τ_c represents some average lifetime, $\eta(T)$ is the solvent viscosity, E_a is the height of the potential barrier, and A is a constant for a given polymer.

The validity of eq 1 has been a topic of research for some time. Experimental techniques that have been applied to this question generally are sensitive to the orientation autocorrelation function of some vector in the polymer molecule, e.g., a C–H bond in a ^{13}C NMR experiment or a transition dipole in an optical experiment. It is assumed that the decay of this correlation function is made possible by conformational transitions. Hence eq 1 is applied to some time τ_c characteristic of the correlation function decay. The assumption of a viscous continuum also implies that the correlation function shape should be independent of solvent.

The results of experimental investigations of eq 1 are varied and difficult to reconcile. Mashimo used dielectric relaxation to study poly(*p*-chlorostyrene) in four low viscosity solvents as a function of temperature.[3] He observed results consistent with eq 1, including a correlation function shape independent of solvent and temperature. One limitation of this study was that the solvent viscosities varied by only a factor of 2. Valeur and Monnerie studied anthracene-labeled polystyrene chains in a mixed-solvent system with time-resolved fluorescence anisotropy measurements.[4] They concluded that "the mean relaxation time varies according to a nonlinear law for low viscosities", in contradiction to the prediction of eq 1. Sasaki and co-workers used the same technique to study anthracene-labeled poly(methyl methacrylate) in a mixed-solvent system.[5] They concluded that the correlation function shape changed significantly with solvent viscosity and that the characteristic times for local dynamics did not scale with viscosity in the high-viscosity regime. Lang and co-workers performed ^{13}C and ^{1}H NMR T_1 measurements on poly(ethylene oxide) in a series of halogenated solvents at one temperature.[6] The correlation times deduced from the NMR measurements varied less strongly than the solvent viscosities. Recently Glowinkowski and co-workers in our laboratory performed ^{13}C NMR measurements on polyisoprene in 10 solvents as a function of temperature.[7] They observed correlation times that were proportional to $\eta^{0.4}$ instead of the $\eta^{1.0}$ dependence predicted by eq 1.

Our laboratory recently published time-resolved optical measurements on dilute solutions of anthracene-labeled polyisoprene in five low-viscosity solvents.[8] The correlation function shapes observed were independent of solvent and temperature. In good solvents, the viscosity and temperature scalings of eq 1 were observed. Systematically different behavior was observed in a Θ-solvent. Since the solvent viscosities varied by only a factor of 3 in this work and other investigators have reported deviations from eq 1 at high and low viscosities, we decided to undertake a study of the dynamics of anthracene-labeled

* Author to whom correspondence should be addressed.
† Present address: Polymers Division, National Institute of Standards and Technology, Gaithersburg, MD 20899.
‡ Present address: Japan Synthetic Rubber Co., Ltd., 100 Kawajiri-Cho, Yokkaichi, Mie 510, Japan.

0024-9297/91/2224-3147$02.50/0

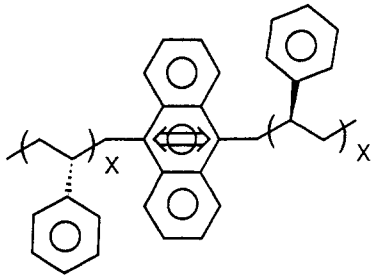

Figure 1. Structure of anthracene-labeled polystyrene. The double-headed arrow indicates the direction of the transition dipole for the chromophore. The chromophore is located approximately in the middle of the polymer chain.

polystyrene over a wide range of solvent viscosities. Six solvents were used in the study reported here, with viscosities varying by more than 2 decades, a considerably larger range than that studied in any other laboratory.

The results presented here indicate that Kramers' approach (eq 1) provides a reasonably accurate description of the local dynamics of anthracene-labeled polystyrene in six solvents, over a wide range of temperatures and viscosities. Consistent with our previous study of anthracene-labeled polyisoprene, an explicable dependence on solvent quality was observed. The relationship between these new results and the results of previous investigations will be addressed.

Experimental Section

Materials. The anthracene-labeled polystyrene was prepared at Nagoya University in a procedure analogous to a synthesis previously described.[9] Briefly, a living polystyrene prepolymer (atactic) was prepared by anionic polymerization. The prepolymer was coupled with 9,10-bis(bromomethyl)anthracene to form a labeled polymer of twice the molecular weight of the prepolymer. The coupling reaction left a substantial fraction of the prepolymer uncoupled; the mixture of coupled polymer and prepolymer was fractionally precipitated to isolate the coupled polymer. The effectiveness of this procedure was checked with GPC using fluorescence detection (excitation 380 nm, fluorescence 430 nm). Fluorescence detection ensures that the GPC detects only the anthracene-labeled polystyrene. Less than 5% of the polystyrene molecules labeled with anthracene were of the molecular weight of the prepolymer and hence uncoupled. This small amount of end-labeled polymer has a negligible effect on the experimental results relative to random errors in the measurements. Substantially all of the chains in the sample contain exactly one chromophore located essentially in the middle of the chain. The structure of the anthracene-labeled polystyrene is shown in Figure 1. Osmotic pressure measurements indicate that M_n = 33 000 for the prepolymer and M_n = 68 000 for the coupled polymer. GPC measurements indicate M_w/M_n = 1.01 for the coupled polymer. The molecular weight of the labeled chains is high enough that overall chain motions can be ignored relative to local chain motions.[10]

Solvents used in these experiments were, in order of increasing viscosity, as follows: 2-butanone (Aldrich, Gold Label, spectrophotometric grade, 99+%), cyclohexane (Aldrich, 99+%), *cis*-decahydronaphthalene (*cis*-decalin, Aldrich, 99%), tripropionin (glycerol tripropanoate, Chem Service, 95%, Lot No. 16-51C), di-*n*-butyl phthalate (Aldrich, Gold label, 99+%), and Aroclor 1248 (Monsanto Chemical Co., Lot No KM502, M_w = 288, average number of chlorines/molecule = 3.9). Aroclor 1248 is a mixture of polychlorinated biphenyls. All solvents were used as received. Figure 2 shows the solvent viscosities at the temperatures where the experiment was performed. Solvent viscosities were obtained from literature sources.[11] With tripropionin, it was necessary to extrapolate the viscosity for 25 °C above the temperature range reported. In this case, an Arrhenius fit was made to the highest temperature data and used for the extrapolation. We estimate the error in this procedure to be less than 10%. Cyclohexane and *cis*-decalin are relatively poor solvents for polystyrene with

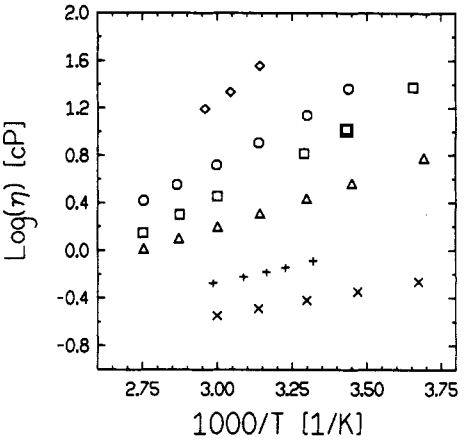

Figure 2. Arrhenius plot of solvent viscosities. Solvent code: 2-butanone (×); cyclohexane (+); *cis*-decalin (△); tripropionin (□); di-*n*-butyl phthalate (○); Aroclor 1248 (◇).

Θ-temperatures of 34.5 and 12.5 °C, respectively.[12] The other solvents are good solvents.

Solutions of labeled polymer were prepared with a polymer concentration of ≤0.15 % w/w. All of the solutions except those in Aroclor 1248 were filtered (0.45 μm) and then processed through several freeze–pump–thaw cycles to remove molecular oxygen. Aroclor 1248 solutions were not filtered or degassed due to high viscosity. We did not observe excessive scattering from the Aroclor solutions, and the fluorescence lifetime was shortened only slightly due to dissolved oxygen. The optical densities (385 nm, 3-mm cells) of all solutions were in the range of 0.02–0.05. The chromophore density was sufficiently low that any contribution to the anisotropy decay curves due to energy transfer could be ignored. Thermal degradation or photodegradation was not observed during the course of any of these experiments.

Experimental Technique. Time-correlated single-photon counting (TCSPC) has been used extensively to measure luminescence lifetimes.[13] When a chromophore is raised to an excited state by absorption of a photon, the probability that a luminescence photon will be emitted at a given time later is given by the excited-state decay function $K(t)$. In a TCSPC experiment, $K(t)$ is measured by building a histogram of arrival times for the emitted photons. The arrival times are clocked relative to the time when a portion of the excitation pulse arrives at a fast photodiode. To monitor the reorientation dynamics of a chromophore, polarized fluorescence decays parallel and perpendicular to the excitation polarization are recorded ($I_\parallel(t)$ and $I_\perp(t)$). Immediately after polarized excitation to a parallel transition, most of the fluorescence will have the same polarization as the excitation pulse. As thermal motions reorient the transition dipoles of the excited chromophores, the ratio of parallel to perpendicular emission will tend toward unity. Applications of the fluorescence anisotropy technique to the study of local polymer dynamics are reviewed in refs 14 and 15.

The polarized emission signals are related to $K(t)$ and the reorientation of the chromophores by:

$$I_\parallel(t) = K(t)[1 + 2r(t)] \tag{2}$$

$$I_\perp(t) = K(t)[1 - r(t)] \tag{3}$$

The anisotropy function $r(t)$ can be extracted from the polarized emission decays by:

$$r(t) = \frac{I_\parallel(t) - I_\perp(t)}{I_\parallel(t) + 2I_\perp(t)} \tag{4}$$

The anisotropy contains information about chromophore reorientation. For the present case where the excitation and emission dipoles are approximately parallel, $r(t)$ is proportional to the second-order orientation autocorrelation function CF(t):

$$r(t) = r(0)\ \mathrm{CF}(t) \tag{5}$$

The correlation function describes the average reorientation of

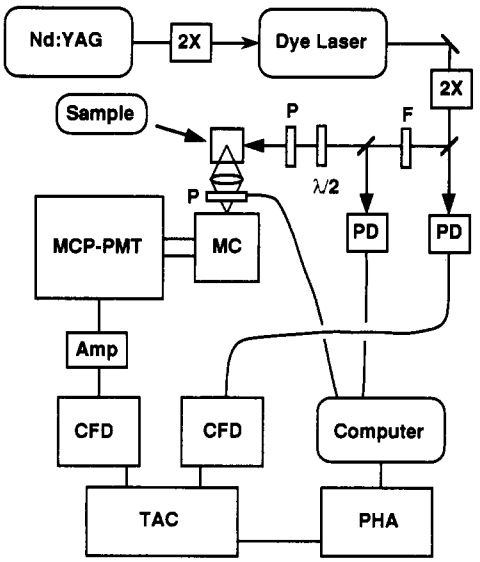

Figure 3. Block diagram of the time-correlated single-photon counting apparatus: MCP-PMT, microchannel plate photomultiplier tube; PD, photodiode; CFD, constant fraction discriminator; TAC, time-to-amplitude converter; PHA, pulse height analyzer; MC, monochromator; 2X doubling crystal; P, polarizer; F, filter; λ/2, half-wave plate.

the transition dipole μ between the times of excitation and emission:

$$CF(t) = \langle P_2(\mu(0)\cdot\mu(t))\rangle \quad (6)$$

In this equation, P_2 is the second Legendre polynomial. Through the use of eqs 1–5, the polarized emission decays allow the unambiguous evaluation of the orientation autocorrelation function of the 9,10-axis of the anthracene chromophore in the labeled chain. Note that this axis is along the chain backbone and that rotation about this axis does not affect the correlation function decay.

Experimental Apparatus. Figure 3 shows a schematic view of our TCSPC apparatus. This system is similar to others described in the literature[16] and is only briefly described here. A frequency-doubled mode-locked Nd:YAG laser pumped a cavity-dumped dye laser. The dye laser produced 1.5-ps pulses (fwhm of the autocorrelation trace) at 770 nm with a repetition rate of 2 MHz. This laser beam was then focused into a doubling crystal, which produced the 385-nm pulses used for sample excitation. A half-wave plate and polarizer were used to adjust the excitation polarization to vertical. The undoubled light was detected by a fast photodiode, which then sent the signal through a constant fraction discriminator to the time-to-amplitude converter (TAC). A small fraction of the 385-nm beam was detected by a slow photodiode so that fluorescence decays could be corrected for long-term laser intensity fluctuations. The fluorescence from the sample was collected and focused through a polarizer (orientation controlled by a stepper motor) into a $^1/_4$-m monochromator set to 410 nm (5-nm band-pass). The grating was masked to reduce the distribution of photon transit times traveling through the monochromator. The output of the monochromator was then directed to a microchannel plate photomultiplier tube (MCP-PMT, Hamamatsu 2809U-01). After amplification, the MCP-PMT signal was sent through a constant-fraction discriminator to the TAC. The TAC was operated in the reverse mode, with the signal from the MCP-PMT acting as the start pulse. The delay between the pulses was analyzed by a pulse height analyzer and recorded as a histogram. A personal computer was used to monitor the laser intensity, store the histogram, and control the analyzing polarizer. The data were subsequently sent to a VAX 8650 for further analysis.

We determined that the differential nonlinearity of the TAC was ≤1.0% for the conditions used in these experiments. The counting rate was kept to ≤0.5% of the excitation rate to prevent pulse pileup. A dilute aqueous solution of nondairy coffee creamer was used as the scattering solution for measuring the instrument response function (IRF). The IRF for all experiments reported here had a fwhm of about 50 ps. As the IRF width is negligible compared with the decay of the anisotropy and the excited-state lifetime, the data were analyzed by using a δ function for the IRF. To check this procedure, we performed an iterative reconvolution fitting procedure with the actual IRF on a few data sets and determined that the fitting parameters changed less than 1%. At the emission wavelength of 410 nm, the detection system had a slight polarization bias; the data was corrected for this bias. The sample temperature was controlled to ±0.1 °C during data acquisition.

Data Collection. For a given sample, six or more pairs of parallel and perpendicular emission decay curves were acquired at a given temperature. This required about 30 min. Each pair of curves was analyzed to obtain the fitted parameters. In addition, the individual parallel curves and individual perpendicular curves were added to give a summed pair of parallel and perpendicular curves. This summed pair was also fit, and the results were compared to the average for the fits of the individual pairs. Both methods gave consistent results for the fit parameters, usually within 1%. On the basis of the results of experiments repeated on different days, we estimate the random error in the fit parameters to be <±10%. The total number of counts at the peak of the summed parallel curves was typically 10^5–10^6.

Data Analysis. We fit the anisotropy decays to two different models of the correlation function: the Hall–Helfand model[17] and the generalized diffusion and loss model[18] (GDL). We consistently found that the GDL provided a better fit to the data, and only these results are reported. Quality of the fits was determined by χ_r^2, a visual examination of the weighted residuals, and the autocorrelation of the weighted residuals. The residuals for the fits to the GDL model were not quite random, but χ_r^2 was typically <1.3 when fitting the anisotropy from individual pairs of parallel and perpendicular curves.

The expression for the anisotropy decay function using the GDL model is

$$r(t) = r(0)\exp(-t/\tau_1)\exp(-t/\tau_2)[I_0(t/\tau_1) + I_1(t/\tau_1)] \quad (7)$$

A standard nonlinear least-squares algorithm was used to fit the three parameters in eq 7: $r(0)$, τ_1, and τ_2. In some cases the decay of the anisotropy function was sufficiently slow that this procedure did not yield reasonable parameters (see below). A fitting procedure that constrained the ratio of τ_2/τ_1 was used when the anisotropy did not decay to <0.05. The correlation time τ_c was used to characterize the average decay time of each correlation function for subsequent analysis. τ_c is simply the integral of the correlation function, given for the GDL model by:

$$\tau_c = \left(\frac{2}{\tau_1\tau_2} + \frac{1}{\tau_2^2}\right)^{-1/2}\left(\frac{1}{\tau_1}\left(\frac{1}{\tau_1} + \frac{1}{\tau_2} + \left(\frac{2}{\tau_1\tau_2} + \frac{1}{\tau_2^2}\right)^{1/2}\right)^{-1} + 1\right) \quad (8)$$

One indication of the quality of the fits obtained by the procedure described is the consistency of the fundamental anisotropy $r(0)$. Since this parameter is related to the angle between the emission and excitation dipoles of the anthracene chromophore, in usual circumstances it should be independent of solvent and temperature. All the fitted $r(0)$ values fell in the range 0.31 ± 0.02, independent of solvent and temperature. This result is different from trends for similar systems discussed in refs 19 and 20. More work is needed to clarify the reasons for this.

Results

In Figure 4 typical polarized fluorescence decays $I_\parallel(t)$ and $I_\perp(t)$ are shown. The sample is a dilute solution of anthracene-labeled polystyrene in cyclohexane at 36.7 °C. Figure 5 shows the anisotropy decay curve for these data calculated with eq 4. The solid line running through the data is the best fit to the anisotropy using the GDL model. The curve at the bottom of the graph is the weighted residuals. The curve in the upper left-hand corner is the autocorrelation of the weighted residuals. The approximately random behavior of the autocorrelation and the residuals, along with the low χ_r^2 (1.21), indicates that the model fits the data reasonably well.

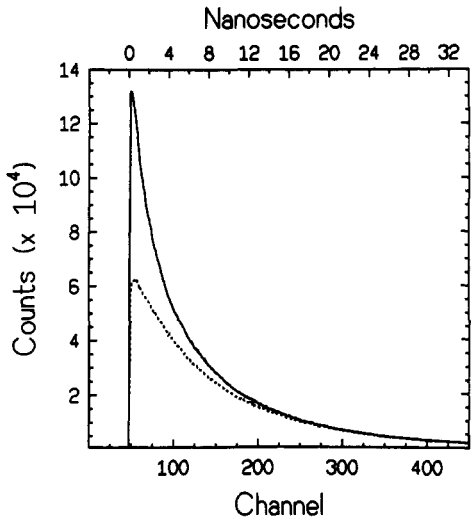

Figure 4. Polarized fluorescence decay curves for a dilute solution of anthracene-labeled polystyrene in cyclohexane (36.7 °C). The two decay curves, $I_{\parallel}(t)$ and $I_{\perp}(t)$, result from detecting fluorescence polarized parallel and perpendicular to the polarization of the excitation. They are shown as solid and dashed lines, respectively. The initial difference between the two curves results from the anisotropic orientational distribution of excited-state chromophores photoselected by the polarized excitation pulse. At longer times, the motion of the polymer backbone causes randomization of this anisotropic distribution and the two curves merge. Eventually both curves decay due to the excited-state lifetime. The resulting anisotropy function from these decay curves is shown in Figure 5.

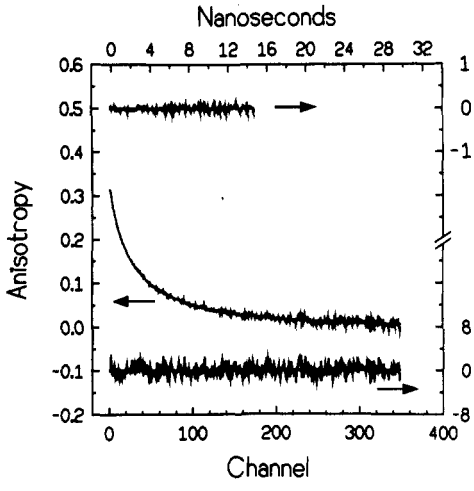

Figure 5. Anisotropy decay curve for anthracene-labeled polystyrene in cyclohexane (data from Figure 4). The smooth line running through the data indicates the best fit using the GDL model: $r(0) = 0.316$, $\tau_1 = 1.30$ ns, $\tau_2 = 13.0$ ns, $\chi_r^2 = 1.21$. The weighted residuals are shown at the bottom of the graph, and the autocorrelation of the weighted residuals is shown in the upper left-hand corner.

In Figure 6 anisotropy curves for four temperatures are plotted for a dilute solution of anthracene-labeled polystyrene in *cis*-decalin. The smooth lines running through the data are fits using the GDL model. The anisotropy decays more slowly at lower temperatures. For the two lowest temperatures the complete decay of the anisotropy cannot be measured in the experimentally available time window. This is not due to any limitation of the apparatus but rather to the fluorescence lifetime of the anthracene chromophore. The experimental window shown corresponds to more than four fluorescence lifetimes; after this time the number of fluorescence photons emitted becomes too small for the anisotropy to be accurately calculated.

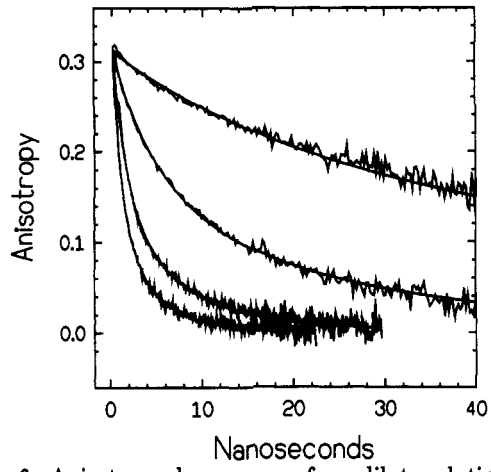

Figure 6. Anisotropy decay curves for a dilute solution of anthracene-labeled polystyrene in *cis*-decalin. The temperatures for these experiments were, from top to bottom, −2.3, 30.2, 60.1, and 90.0 °C. The smooth lines through the data represent the best fits to the GDL model.

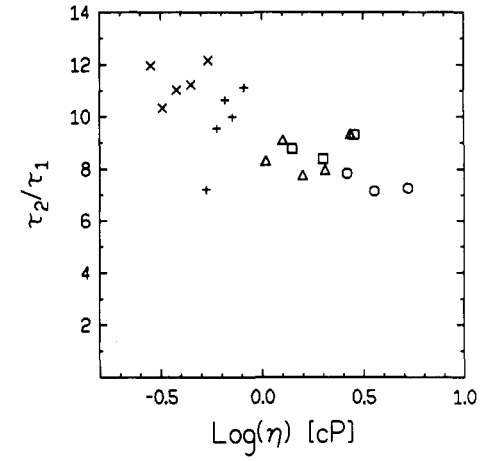

Figure 7. Plot of τ_2/τ_1 against solvent viscosity. This ratio describes the shape of the correlation function and is formed from the fitted values of τ_1 and τ_2. Ratios are shown for all experiments in which the complete correlation function could be measured. Solvent codes are the same as those in Figure 2.

Figure 7 shows the ratio of τ_2/τ_1 obtained from the fitting procedure for all experiments where the anisotropy decay was essentially complete; i.e., the anisotropy decayed to <0.05 in the experimentally available time window. We are confident that under these conditions the shape of the correlation function (which is determined by the ratio τ_2/τ_1) can be accurately extracted from the experimental data. We verified this by taking several anisotropy decays, which were essentially complete, and systematically eliminating data points for the longest times. The fit parameters were stable until the anisotropy did not decay below 0.05; at this point a significant change in the ratio τ_2/τ_1 was observed. This is another indication that the GDL model does not provide an ideal fit to the data.

Figure 7 shows that the correlation function shape is roughly constant, independent of solvent and temperature. GDL correlation function decays with $\tau_2/\tau_1 = 12$ and $\tau_2/\tau_1 = 7$ have quite similar shapes. If these two decays are compared for equal values of τ_c, they differ by at most 0.05 at any time (initial value is 1.0).

For the cases where the complete anisotropy decay is not observed in the experimental time window (such as the lowest temperature shown in Figure 6), we are left with a question as to what information about the correlation function can be reasonably extracted. It is

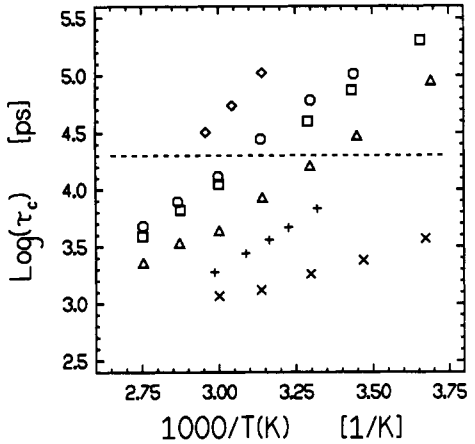

Figure 8. Arrhenius plot of correlation times for all solvents and temperatures. The correlation time is the average time for rotational reorientation of the anthracene label in the polystyrene chain. Data points above the dashed line were determined by using the constrained fitting procedure described in the text. Solvent codes are the same as those in Figure 2.

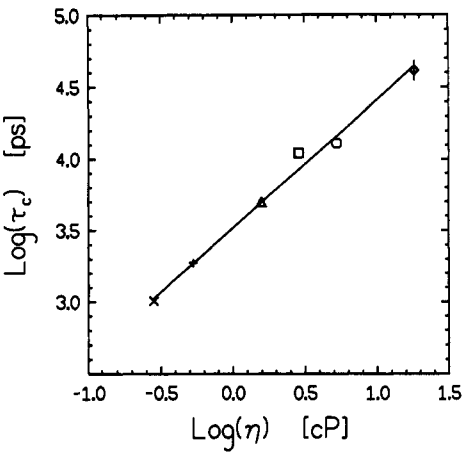

Figure 9. log–log plot of τ_c against solvent viscosity at 60 °C. The line represents the best linear least-squares fit to the data and has a slope of 0.9. The prediction of Kramers' equation is a slope of 1.0. Error bars are the size of the data points except where shown. Solvent codes are the same as those in Figure 2.

pointless to attempt to measure the shape of the correlation function under these conditions since an important part of the correlation function is not observed. However, it is possible to estimate the average decay time of the correlation function τ_c if a reasonable guess can be made about the shape of the correlation function. Figure 7 provides a means for making such a reasonable guess. Figure 7 shows that when the complete decay of the anisotropy is observed, the shape of the correlation function is roughly constant, independent of solvent and temperature. A slight dependence on the solvent viscosity is observed in the figure. We used an average of the τ_2/τ_1 values shown in Figure 7 to constrain the fitting procedure for those cases when the anisotropy did not decay to <0.05. In order to assess the error associated with this approximation, for a few curves, we fit a series of different τ_2/τ_1 values in the range from 7 to 12. The τ_c values extracted from these fits varied by at most 20%.

In Figure 8 we present the average decay time τ_c for all samples and temperatures. The τ_c values span a range from 1 to 200 ns. Above the dashed line, the shape of the correlation function was constrained as described in the previous paragraph. On the basis of repeated measurements on different days, we regard the random error in τ_c to be ±10% for unconstrained fits and ±15% for constrained fits.

Discussion

Viscosity Dependence. Figure 7 indicates that the shape of the correlation function is roughly constant, independent of solvent or temperature. Thus, we can make an unambiguous test of Kramers' equation (eq 1) using the correlation time τ_c to characterize the correlation function decay. Figure 9 shows a comparison of log τ_c with log η for data obtained at 60 °C. Kramers' equation predicts that the data should fall on a straight line with slope 1. The data fall reasonably well on a straight line; the slope of the line that best fits the data is 0.90 ± 0.05. Given the specified error in the experimental measurements, this result is reasonably consistent with Kramers' prediction. Note that almost 2 orders of magnitude in viscosity are represented in Figure 9.

The data shown in Figure 9 were collected at 60 °C, the highest temperature for which we have correlation times in all six solvents. We chose data collected at this temperature for the figure for two reasons. First, all but one of the τ_c values at this temperature could be obtained without resorting to the constrained fitting procedure. Second, this temperature is as far as possible from the Θ-temperature of cyclohexane and *cis*-decalin; this minimizes any possible influence of solvent quality in the comparison. The correlation time for the Aroclor 1248 solution was unavailable at exactly 60 °C, so an interpolated point was taken from a least-squares fit to the data shown in Figure 8.

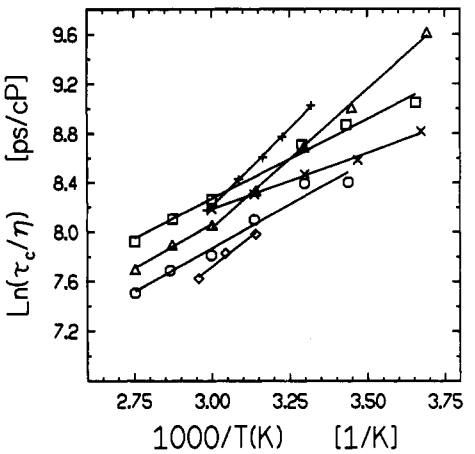

Figure 10. Arrhenius plot of correlation times reduced by the solvent viscosity at the temperature at which the experiment was performed. The lines are linear least-squares fits to the data for each solvent. The apparent activation energies for the Θ-solvents (*cis*-decalin and cyclohexane) are significantly greater than those for the good solvents. Solvent codes are the same as those in Figure 2.

Temperature Dependence. The data shown in Figure 9 represent a test of Kramers' equation using data from only one temperature. We compare the data from all solvents and temperatures with the prediction of Kramers' equation in Figure 10. The correlation time divided by the solvent viscosity at the measurement temperature has been plotted versus the inverse temperature. Best fit lines for data from each solvent are also shown; the *cis*-decalin data have been fit to two linear regions, as the data appear to show a break about 60 °C (see below).

Kramers' prediction for Figure 10 is a single line for all solvents, with the slope proportional to the potential energy barrier E_a. To a first approximation, this prediction is correct. As shown in Figure 8, the correlation times differ by almost a factor of 100 before scaling by the solvent

Table I
Apparent Activation Energies

solvent	E_a, kJ/mol	solvent	E_a, kJ/mol
cyclohexane	21 ± 2	di-*n*-butyl phthalate	12 ± 2
cis-decalin (low *T*)	19 ± 2	tripropionin	11 ± 2
Aroclor 1248	16 ● 5	2-butanone	8 ± 2
cis-decalin (high *T*)	12 ± 4		

viscosity. The deviation from a single line in Figure 10 is only a factor of 2.

Activation Energies. Using Kramers' equation and Figure 10, we can calculate the apparent activation energies for all six solvents. The results of this calculation are shown in Table I. In a previous optical study of the local segmental dynamics of polyisoprene,[8] we noted a systematic dependence of the apparent activation energy upon the solvent quality; for high molecular weight chains, apparent activation energies for local dynamics were higher for a Θ-solvent than for good solvents. The data in Table I also fit this pattern; activation energies are highest in the two Θ solvents (for *cis*-decalin, the low-temperature region is closest to the Θ-temperature). The data for *cis*-decalin appear to show a transition from a region influenced by the Θ-temperature to a region with an apparent activation energy similar to the good solvents. For the last five entries in Table I (good solvents), a reasonably consistent activation energy of 11 ± 3 kJ/mol is obtained. (The error bar on the activation energy in Aroclor is large enough to make this solvent irrelevant to the preceding discussion.)

The dependence of the apparent activation energy upon solvent quality can be explained by considering the local concentration of chain segments about the chromophore.[8] In a Θ-solvent, changes in global chain dimensions occur with temperature. The expansion of the chain with increasing temperature decreases the local segment concentration and thus increases the rate of conformational transitions. In addition, there is an increase in the rate of conformational transitions due to the fact that more thermal energy is now available relative to the potential barrier height. This second effect is the normal activation energy term. In a Θ-solvent, the first effect is an additional contribution to the temperature dependence of the dynamics, which makes the apparent activation energy larger than the height of the potential barrier. Thus, the best estimate of the average barrier height for local dynamics in polystyrene from these experiments is 11 kJ/mol.

An alternative explanation for the different dynamics noted in good solvents and Θ-solvents is found in recent computer simulations by Kovac and co-workers.[21] They simulated chain dynamics as a function of solvent quality and noticed that local modes slowed near the Θ-condition. They concluded that an increase in the local segment density such as discussed above probably cannot explain this observation for their system. Rather, they proposed that an observed increase in the lifetime of pair contacts explains the slower dynamics.

Comparison to Other Work. There has been a previous study of anthracene-labeled polystyrene using a nanosecond optical technique by Viovy and co-workers.[18] Under conditions where the results of this previous study can be compared with the results presented here, the agreement is good. Viovy and co-workers report results for dilute solutions of polystyrene in mixtures of tripropionin and ethyl acetate. They found that the GDL model provided a better fit to the data than the Hall–Helfand model, with ratios of τ_2/τ_1 about 10 for the GDL model. This agrees quantitatively with our results. They found a τ_c of 46 ns at 25 °C when the solvent was 94% tripropionin/6% ethyl acetate. Interpolating our results for 95% tripropionin, we estimate a τ_c of 51 ± 5 ns at 25 °C. Viovy and co-workers reported $r(0)$ values of about 0.22, in contrast to the values of 0.31 reported here. This is consistent with the fact that the excitation and emission wavelengths were nearer the origin transition in our work.

Valeur and co-workers used time-resolved optical measurements to determine the activation energy for anthracene-labeled polystyrene to be between 4 and 14 kJ/mol, depending upon solvent conditions.[22] These results were obtained for a mixed-solvent system and thus cannot be directly compared to any of the solvents studied here. Nevertheless, the lowest values obtained by Valeur and co-workers are difficult to reconcile with the results presented here. It was shown later that the functional form used for the correlation function in these experiments does not accurately fit the data.[18,23] This is a possible explanation for the difference between ref 22 and the present work.

Bullock and co-workers used electron spin resonance to study local dynamics of spin-labeled polystyrene.[24] Their results agree semiquantitatively with those presented here. In good solvents, activation energies of 9 kJ/mol were reported. Higher values were observed in a Θ-solvent. References 22 and 24 both report that correlation times reduced by solvent viscosity were larger in Θ-solvents than in good solvents. This is also in good agreement with our results.

Sasaki and co-workers have utilized time-resolved fluorescence anisotropy techniques to examine the dynamics of anthracene-labeled poly(methyl methacrylate).[5] They observed that the shape of the correlation function was constant up to a viscosity of about 4 cP. In this same region, the correlation time scaled linearly with the viscosity. Above 4 cP, this scaling broke down and the shape of the correlation function determined by the fitting procedure was observed to change significantly. In our results on anthracene-labeled polystyrene, we observe a roughly constant correlation function shape and correlation times that scale with the viscosity up to 18 cP. It is possible that the different conclusions reported for the polystyrene and poly(methyl methacrylate) systems reflect differences in specific polymer/solvent interactions in these two systems. It is also possible that the observed differences are due to different fitting procedures used in the two studies. Sasaki and co-workers did not use a constrained fitting procedure for any solutions, while we used constrained fitting for solutions with viscosities larger than about 5 cP. It is likely that the results from these two studies would be more similar if the same fitting procedure had been used. Indeed, unconstrained fits of our data when the complete decay of the correlation function was not observed gave τ_2/τ_1 values significantly different from those reported in Figure 7. This was true both for high-viscosity data and low-viscosity data from which we had artificially removed data points from the end of the decay.

It is not possible to determine unambiguously whether the fitting procedure used in this study or the one used by Sasaki and co-workers is more likely to yield the correct results. Whenever the complete correlation function decay is not observed in an experiment, some uncertainty must be expected in conclusions about the shape of the function. We prefer the procedure used in this paper as being less likely to lead to artifacts. Unless the model function is a perfect fit to the data, fitting without constraints will always lead to changes in the shape of the correlation function as less of it is observed. The conclusions obtained

from the constrained fitting procedure also seem to be more simple and reasonably consistent with theory.

As mentioned in the Introduction, a pioneering time-resolved optical study on anthracene-labeled polystyrene by Valeur and Monnerie concluded that mean relaxation times varied nonlinearly with viscosity at low viscosities.[4] Our results on the same type of labeled polymer (Figure 9) show no evidence of this. We believe this difference is due to the difficulty of performing early time-resolved measurements. Subsequent work from the same laboratory found significantly different mean relaxation times for the same polymer/solvent system.[18]

Recent NMR measurements performed in our laboratory[7] have clearly shown that local dynamics in polyisoprene, as determined by NMR, scale with $\eta^{0.4}$ as opposed to the $\eta^{1.0}$ dependence predicted by Kramers' equation. Previous NMR measurements by Lang and co-workers[6] on poly(ethylene oxide) show an $\eta^{0.7}$ dependence.[7] Reference 7 presents an extensive discussion of the origin of the apparent power law dependence of τ_c on η and on the relationship of the NMR measurements to optical measurements. Consistent with the theory of Grote and Hynes,[25] local polymer motions that are small enough and involve rapid crossing of a potential barrier may experience a friction that is less than that expected based on the macroscopic viscosity. Under these conditions, the viscosity exponent will be less than 1, while for larger and slower motions an exponent of 1 is expected. The relatively large size of the side groups for polystyrene as opposed to polyisoprene, and the size of the chromophore itself, argues for a viscosity exponent near 1 in the optical experiment, as observed.

Conclusions

The major conclusion of this paper is that Kramers' theory provides a quite reasonable description of the local segmental dynamics of anthracene-labeled polystyrene. The predicted viscosity scaling holds remarkably well over almost 2 decades in viscosity. Potential barrier heights are independent of solvent for good solvents. Larger apparent activation barriers were observed near the Θ-temperature in Θ-solvents. While this feature is not predicted by Kramers' theory, it is explicable in terms of changes in segment/segment interactions associated with the Θ-temperature. All these points are consistent with an earlier study from our laboratory on anthracene-labeled polyisoprene.[8]

The view of the solvent as a viscous continuum is not rigorously supported by the experimental results on two points. First, the observed scaling of the correlation time with the viscosity is not 1.00 within experimental error. Second, a slight dependence of the shape of the correlation function on the solvent viscosity was observed. This implies that the precise details of the local motions are not the same in different environments, even after the viscosity is used to scale the time scales of the motions.

Two more general caveats to the above conclusion also need to be stated: (1) Different experimental techniques are sensitive to different types of local dynamics. Techniques such as NMR that sense very rapid motions occurring on the scale of 1 or 2 repeat units may not follow the viscosity dependence of Kramers' equation. These deviations have been reported in NMR studies on two systems. Optical techniques, sensing motions over a slightly longer length scale (≈5–10 repeat units), are more likely to be described by Kramers' equation. (2) Relatively nonpolar systems were studied in this work. We expect that Kramers' approach may fail dramatically for more polar polymer/solvent systems or systems where hydrogen bonding occurs.

Acknowledgment. This research was supported by the National Science Foundation (Grants DMR-8822076 and CHE-8804083). We thank the Graduate School at the University of Wisconsin for matching funds used in the purchase of the TCSPC instrument. M.D.E. thanks the Alfred P. Sloan Foundation for fellowship support. M. Yamamoto is acknowledged for helpful discussions.

References and Notes

(1) Kramers, H. A *Physica* **1940**, *7*, 284.
(2) Helfand, E. *J. Chem. Phys.* **1971**, *54*, 4651.
(3) Mashimo, S. *Macromolecules* **1976**, *9*, 91.
(4) Valeur, B.; Monnerie, L. *J. Polym. Sci., Polym. Phys. Ed.* **1976**, *14*, 11.
(5) Sasaki, T.; Yamamoto, M.; Nishijima, Y. *Macromolecules* **1988**, *21*, 610.
(6) Lang, M. C.; Laupretre, F.; Noel, C.; Monnerie, L. *J. Chem. Soc., Faraday Trans. 2* **1979**, *75*, 349.
(7) Glowinkowski, S.; Gisser, D. J.; Ediger, M. D. *Macromolecules* **1990**, *23*, 3520.
(8) Waldow, D. A.; Johnson, B. S.; Hyde, P. D.; Ediger, M. D.; Kitano, T.; Ito, K. *Macromolecules* **1989**, *22*, 1345.
(9) Hyde, P. D.; Waldow, D. A.; Ediger, M. D.; Kitano, T.; Ito, K. *Macromolecules* **1986**, *19*, 2533.
(10) See the discussion of this point in ref 8. Including a correction for overall chain motion would increase τ_c values by about 7% and τ_2 values by about 12%. We have not included these corrections since they are about the same size as the random errors in the results.
(11) Solvent viscosities were obtained from the following references. (a) 2-Butanone: *International Critical Tables*; McGraw-Hill: New York, 1930; Vol. 7, p 215. (b) Cyclohexane: Stephan, K.; Lucas, K. *Viscosity of Dense Fluids*; Plenum Press: New York, 1979; p 87. (c) *cis*-Decalin: Viswanath, D. S.; Natarajan, G. *Data Book of the Viscosity of Liquids*; Hemispheric Publishing Co.: New York, 1989; p 207. (d) Tripropionin: Viovy, J. L. *J. Phys. Chem.* **1985**, *89*, 5465. (e) Di-*n*-butyl phthalate: Barlow, A. J.; Lamb, J.; Matheson, A. J. *Proc. R. Soc. London* **1966**, *292*, 322. (f) Aroclor 1248: Harris, J. S. Product Engineering, Dec 1954, p 163. Stokich, T. M. Ph.D. Thesis, University of Wisconsin, 1988. Merchak, P. A. Ph.D. Thesis, University of Wisconsin, 1987. Viscosity data for Aroclor 1248 were combined in the manner described in ref 7.
(12) Berry, G. C. *J. Chem. Phys.* **1966**, *44*, 4550. Brandrup, J.; Immergut, E. H. *Polymer Handbook*, 2nd ed.; John Wiley and Sons: New York, 1975; p IV-166.
(13) See, for example: O'Conner, D. V.; Phillips, D. *Time-Correlated Single Photon Counting*; Academic Press: London, 1984.
(14) Monnerie, L.; Viovy, J. L. In *Photophysical and Photochemical Tools in Polymer Science*; Winnik, M. A., Ed.; Reidel: Dordrecht, The Netherlands, 1986; pp 193–224.
(15) Ediger, M. D. *Annu. Rev. Phys. Chem.*, in press.
(16) Chang, M. C.; Courtney, S. H.; Cross, A. J.; Gulotty, R. J.; Petrich, J. W.; Fleming, G. R. *Anal. Instrum.* **1985**, *14*, 433. This entire issue is related to time-correlated single-photon counting.
(17) Hall, C. K.; Helfand, E. *J. Chem. Phys.* **1982**, *77*, 3275.
(18) Viovy, J. L.; Monnerie, L.; Brochon, J. C. *Macromolecules* **1983**, *16*, 1845.
(19) Veissier, V.; Viovy, J. L.; Monnerie, L. *J. Phys. Chem.* **1989**, *93*, 1709.
(20) Viovy, J. L. *J. Phys. Chem.* **1985**, *89*, 5465.
(21) Downey, J. P.; Kovac, J. *Macromolecules* **1990**, *23*, 3013. Sorensen, C. C.; Kovac, J. submitted for publication in *Macromolecules*.
(22) Valeur, B.; Kasparyan, N.; Monnerie, L. *26th Int. Symp. Macromol. Mainz* **1979**, *2*, 989.
(23) The same functional form as in ref 4 was used. Monnerie, L., private communication.
(24) Bullock, A. T.; Cameron, G. G.; Smith, P. M. *J. Chem. Soc., Faraday Trans. 2* **1974**, *70*, 1202.
(25) Grote, R. F.; Hynes, J. T. *J. Chem. Phys.* **1980**, *73*, 2715. Also see: Bagchi, B.; Oxtoby, D. W. *J. Chem. Phys.* **1983**, *78*, 2735.

Registry No. Polystyrene, 9003-53-6; 2-butanone, 78-93-3; cyclohexane, 110-82-7; *cis*-decahydronaphthalene, 493-01-6; tripropionin, 139-45-7; dibutyl phthalate, 84-74-2; Aroclor 1248, 12672-29-6.